Neuron, Vol. 44, 779–793, December 2, 2004, Copyright ©2004 by Cell Press

Rho GTPases Regulate Axon Growth through Convergent and Divergent Signaling Pathways

Julian Ng[1,*] and Liqun Luo*
Department of Biological Sciences
Stanford University
Stanford, California 94305

Summary

Rho GTPases are essential regulators of cytoskeletal reorganization, but how they do so during neuronal morphogenesis in vivo is poorly understood. Here we show that the actin depolymerization factor cofilin is essential for axon growth in *Drosophila* neurons. Cofilin function in axon growth is inhibited by LIM kinase and activated by Slingshot phosphatase. Dephosphorylating cofilin appears to be the major function of Slingshot in regulating axon growth in vivo. Genetic data provide evidence that Rho or Rac/Cdc42, via effector kinases Rok or Pak, respectively, activate LIM kinase to inhibit axon growth. Importantly, Rac also activates a Pak-independent pathway that promotes axon growth, and different RacGEFs regulate these distinct pathways. These genetic analyses reveal convergent and divergent pathways from Rho GTPases to the cytoskeleton during axon growth in vivo and suggest that different developmental outcomes could be achieved by biases in pathway selection.

Introduction

The precise wiring of neural circuits depends on the ability of developing neurons to extend axons and dendrites to their correct targets. To achieve this, developing axons and dendrites elaborate growth cones, which exhibit highly motile actin-based structures that reorganize in response to extracellular cues. Rho GTPases, including Rho, Rac, and Cdc42, are key proteins in transducing signals from extracellular cues to the actin cytoskeleton. Rho GTPases regulate multiple aspects of growth cone behavior, including growth, retraction, pausing, turning, and branching. Many extracellular cues that regulate neuronal morphogenesis exert their effects by modulating Rho GTPase signaling through interactions with positive regulators (RhoGEFs), negative regulators (RhoGAPs), Rho GTPases themselves, or downstream effectors (Luo, 2000).

Rho GTPases activate diverse downstream pathways that regulate distinct aspects of cytoskeletal events, such as actin polymerization, depolymerization, cross-linking, anchoring, and myosin motor activities (Pollard et al., 2000; Etienne-Manneville and Hall, 2002). However, which downstream pathways play essential roles during neuronal development in vivo, what aspects of morphogenesis they control, and how different signaling pathways are coordinated remain largely unknown. To address these questions, we are taking a genetic approach, using *Drosophila* neuronal morphogenesis as a model. We recently showed that the Rho family GTPases Rac1, Rac2, and Mtl are essential for axon growth, guidance, and branching (Ng et al., 2002). Here we address how Rho GTPases are linked to the actin cytoskeletal machinery during axon growth. We find that cofilin regulation is a critical step.

From yeast to mammals, cofilin plays an essential morphogenetic role by promoting the rapid turnover of actin filaments through severing filamentous actin (F-actin) and depolymerizing actin filaments from the pointed ends (Bamburg, 1999). Mutations in the *twinstar* (*tsr*) gene, which encodes the unique *Drosophila* homolog of cofilin, result in neuroblast proliferation, spermatogenesis, and defects in epithelial morphogenesis (Gunsalus et al., 1995; Chen et al., 2001). In mammalian cells, cofilin activity is inhibited by phosphorylation at serine 3 (Morgan et al., 1993; Agnew et al., 1995), which is mediated by LIM kinase (LIMK) (Arber et al., 1998; Yang et al., 1998). LIMK is activated through phosphorylation by p21-activated kinase (Pak) or Rho-associated kinase (Rok, also named Rho kinase or ROCK), effector kinases for Rac/Cdc42 or Rho, respectively (Edwards et al., 1999; Maekawa et al., 1999). In *Drosophila*, one LIMK gene has been found which can also phosphorylate cofilin at serine 3 (*LIMK1*-Flybase) (Ohashi et al., 2000), but how LIMK1 is regulated is unknown. Cofilin is dephosphorylated by Slingshot phosphatase (Ssh) (Niwa et al., 2002). *Drosophila ssh* mutants exhibit defects in epithelial morphogenesis that are characterized by high levels of F-actin and cofilin phosphorylation, suggesting that Ssh regulates actin dynamics through cofilin dephosphorylation.

The function and regulation of cofilin in neuronal morphogenesis in vivo has not been reported. Here we show that loss of cofilin results in severe axon growth defects in *Drosophila* neurons. Cofilin function is positively regulated by Ssh phosphatase and negatively regulated by LIMK during axon growth. Cofilin dephosphorylation appears to be the major function of Ssh, as axon growth defects in *ssh* mutant neurons are suppressed by expressing active forms of cofilin. We provide genetic evidence that both the Rho-Rok and the Rac/Cdc42-Pak pathways positively regulate *Drosophila* LIMK. Importantly, while the LIMK pathway acts to inhibit axon growth, we find that Rac also signals through a Pak-independent pathway that acts antagonistically to LIMK to promote axon growth. Furthermore, two distinct RacGEFs appear to be selectively engaged to regulate these different pathways. These genetic results indicate that multiple Rho GTPase signaling pathways converge on a common downstream target, cofilin, to regulate axon growth. At the same time, Rho GTPases also regulate divergent downstream pathways that act in an antagonistic fashion to coordinate growth cone motility.

Results

To analyze the role of candidate proteins involved in Rho GTPase signaling and neuronal morphogenesis, we

*Correspondence: lluo@stanford.edu (L.L.); julian.ng@kcl.ac.uk (J.N.)
[1]Present address: MRC Centre for Developmental Neurobiology, New Hunt's House, Guy's Campus, London SE1 1UL, United Kingdom.

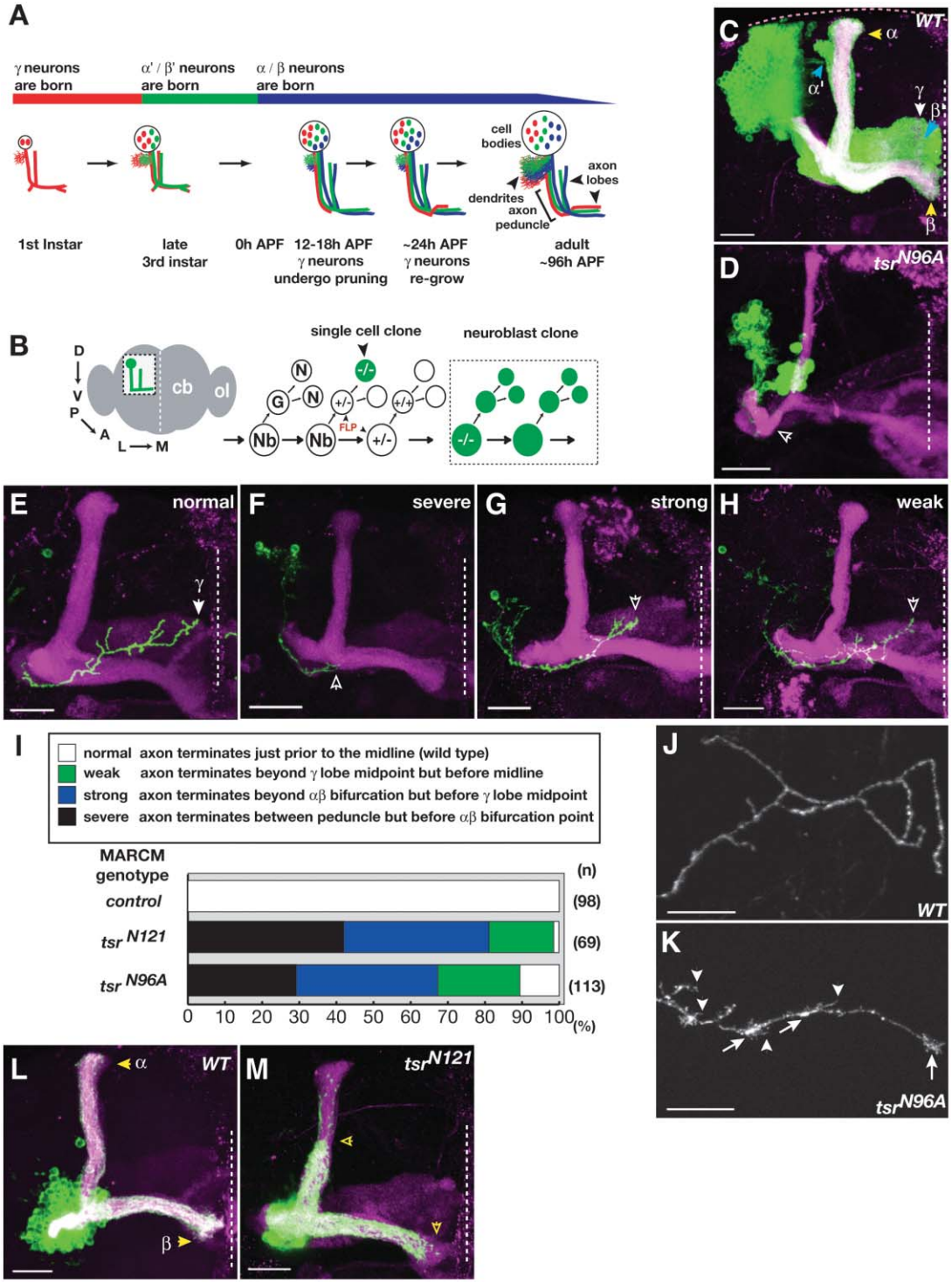

Figure 1. Cofilin/Twinstar Is Required for Neuroblast Proliferation and Axon Growth

(A) Schematic summary of mushroom body (MB) neuronal development (Lee et al., 1999). APF, after puparium formation. (B) Schematic of the *Drosophila* whole brain at the adult stage and MB neuroblast division pattern. The boxed region shows the location of the MB neurons in the left hemisphere of the central brain (cb). The arrows show the overall trajectory of all MB axons extending from the posterior dorsal cell bodies and projecting anteriorally, ventrally, and then turning toward the midline. All MB images shown in this paper correspond to the left hemisphere (boxed region) in the same orientation as the schematic brain. Dashed white lines in all images indicate the midline. D, dorsal; V, ventral; P, posterior; A, anterior; L, lateral; M, midline; ol, optic lobe. MB neuroblasts (Nb) undergo asymmetric division to generate ganglion mother cells (G) that divide once more to generate two postmitotic neurons (N). FLP-induced mitotic recombination could generate homozygous mutant (−/−) neuroblast clones (boxed) or single-cell MB clones (large arrowhead) that are positively labeled by MARCM. (C and D) MB neuroblast MARCM clones for wild-type (C) or tsr^{N96A} (D). A typical adult wild-type neuroblast clone generated from newly hatched larvae

used the mushroom body (MB) neurons in the *Drosophila* central brain as a model. The adult MB is composed of three sets of neurons (γ, α′/β′, and α/β) sequentially derived from common neuroblast precursors (Lee et al., 1999; Figures 1A and 1B). Each MB neuron extends a primary neurite that gives rise to dendritic branches near the cell body and a single axon that projects anteriorly and ventrally through the peduncle. Each axon of the α′/β′ or α/β neurons bifurcates to form a dorsal and a medial branch, whereas each γ neuron has only a medial branch (Figure 1A). All axons terminate either medially at the proximity of the midline (for medial projections) or close to the anterior dorsal cortex (for dorsal projections) (Figure 1C).

To analyze the functions of candidate genes, we used the MARCM system (Lee and Luo, 1999) to generate wild-type or homozygous mutant single-cell or neuroblast clones that are positively labeled (Figure 1B). Neuroblast clones allow us to examine the gross behavior of a large clone of mutant neurons and to assess the role of a given gene in cell proliferation, whereas single-cell clones enable finer resolution of axon morphology of mutant neurons.

Cofilin/Twinstar Is Required for MB Neuroblast Proliferation and Axon Growth

We have previously shown that the Rho GTPases are essential in regulating the morphogenesis of MB neurons (e.g., Ng et al., 2002). What are the effector pathways that lead to cytoskeletal regulation in vivo? One candidate pathway is cofilin regulation. Cofilin and the related actin depolymerization factor (ADF) in mammals have a single homolog in *Drosophila*, encoded by the *tsr* locus (Gunsalus et al., 1995). To examine cofilin function, we generated neuroblast clones in newly hatched larvae and examined MB clones in adults. Wild-type MB neuroblast clones generated under this condition typically contain approximately 400 MB neurons composed of all three classes (Figures 1A and 1C). In contrast, $tsr^{-/-}$ neuroblast clones for two different null alleles of *tsr* (tsr^{N96A} and tsr^{N121}) contain 15 to 30 neurons (Figure 1D, n = 8 for both alleles). This cell proliferation defect is consistent with previous findings that *tsr* is essential for cytokinesis in the *Drosophila* brain (Gunsalus et al., 1995).

In addition to cell proliferation defects, $tsr^{-/-}$ neuroblast clones also exhibited severe axon growth defects, as a majority of mutant neurons failed to extend their axons beyond the peduncle (Figure 1D, open arrowhead). To study axon growth at a higher resolution, we analyzed $tsr^{-/-}$ single-cell clones of γ neurons. At the adult stage, all wild-type γ neurons extend their axons to the end of the γ lobe, to the proximity of the midline (Figure 1E, quantification in Figure 1I). However, 30%–40% of $tsr^{-/-}$ axons did not enter the medial lobe (stopping before the α/β branching point) (Figures 1F and 1I, classified as "severe"), another 35%–40% failed to extend beyond the midpoint of the γ lobe (Figures 1G and 1I, "strong"), and an additional 15%–20% failed to reach the end of the γ lobe (Figures 1H and 1I, "weak"). Thus, axon growth requires cofilin cell-autonomously.

When examined at a higher magnification, $tsr^{-/-}$ axons exhibited characteristic morphological defects. In contrast to the relatively uniform axon shafts and terminals in wild-type neurons (Figure 1J), most $tsr^{-/-}$ axons displayed multiple small protrusions and swellings along the shaft and at the terminal (Figure 1K), reminiscent of filopodia and lamellipodia normally associated with developing growth cones. These observations are consistent with the idea that actin depolymerization is required to turn over transient growth cone filopodia and lamellipodia during axon growth and that loss of such turnover results in growth defects.

We also tested the role of *tsr* in MB α/β neurons by generating neuroblast clones that contain only α/β neurons (Figure 1A). Wild-type α/β neurons typically extended dorsal and medial projections that end at the midline and dorsal cortex (Figure 1L, n > 10). In contrast, most $tsr^{-/-}$ α/β axons failed to extend fully to the midline or to the dorsal cortex (Figure 1M, 4 of 6 $tsr^{-/-}$ neuroblast clones). Therefore, α/β neuron axon growth also requires cofilin.

Cofilin Function in Cell Proliferation and Axon Growth Is Regulated by Phosphorylation

Cofilin function is regulated by phosphorylation in higher eukaryotes. Cofilin is active in a dephosphorylated state and becomes inhibited once it is phosphorylated at serine 3. Mutational analyses show that changing serine 3 to an alanine (S3A) generates a constitutively active cofilin, whereas changing serine 3 to a glutamic acid (S3E) inhibits cofilin activity (Agnew et al., 1995; Abe et al., 1996). To test whether cofilin phosphorylation plays an essential role in vivo, we generated transgenic flies that express wild-type, S3A, or S3E forms of cofilin under the control of the GAL4-UAS expression system (Brand and Perrimon, 1993). Overexpression of these transgenes in wild-type MB neurons did not result in gross axon or cell proliferation defects (data not shown).

Then, using the MARCM system, we performed transgenic rescue experiments by expressing wild-type, S3A, or S3E cofilin in $tsr^{-/-}$ clones. We first examined the

contains approximately 400 neurons that consist of γ, α′/β′, and α/β neurons, as indicated. In contrast, $tsr^{-/-}$ neuroblast clones contain much fewer cells. The image in (D) shows two neuroblast clones, each with 15 to 30 cells. Dashed pink line in (C) indicates the dorsal cortex. Filled arrowheads indicate the termination of wild-type axons. Open arrowheads indicate arrested axon growth in mutant neurons. (E–H) Single-cell clones of γ neurons for wild-type (E) or tsr^{N121} (F–H), representing severe, strong, or weak axon growth defects. Filled white arrowheads indicate the termination of wild-type γ axons; open arrowheads indicate axon growth defects in mutant γ axons. (I) Quantification of axon growth defects in *tsr* mutant single-cell clones of γ neurons. n, number of single-cell clones examined. (J and K) Higher magnification of adult wild-type (J) or tsr^{N96A} axon termini (K) single-cell γ neurons. Arrows in (K) indicate lamellipodia-like structures; arrowheads indicate filopodia-like structures. These structures are absent in wild-type axons (J). (L and M) Images of neuroblast clones containing only α/β neurons of wild-type (L) or tsr^{N121} (M) neurons. Scale bars, 20 μm (C–H, L, and M), 10 μm (J and K). All images in this and subsequent figures are Z projections of confocal sections. Green, neuroblast or single-cell MARCM clones (sometimes multiple single-cell clones) immunostained with anti-CD8 antibodies; magenta, FasII staining of all MB γ and α/β axons.

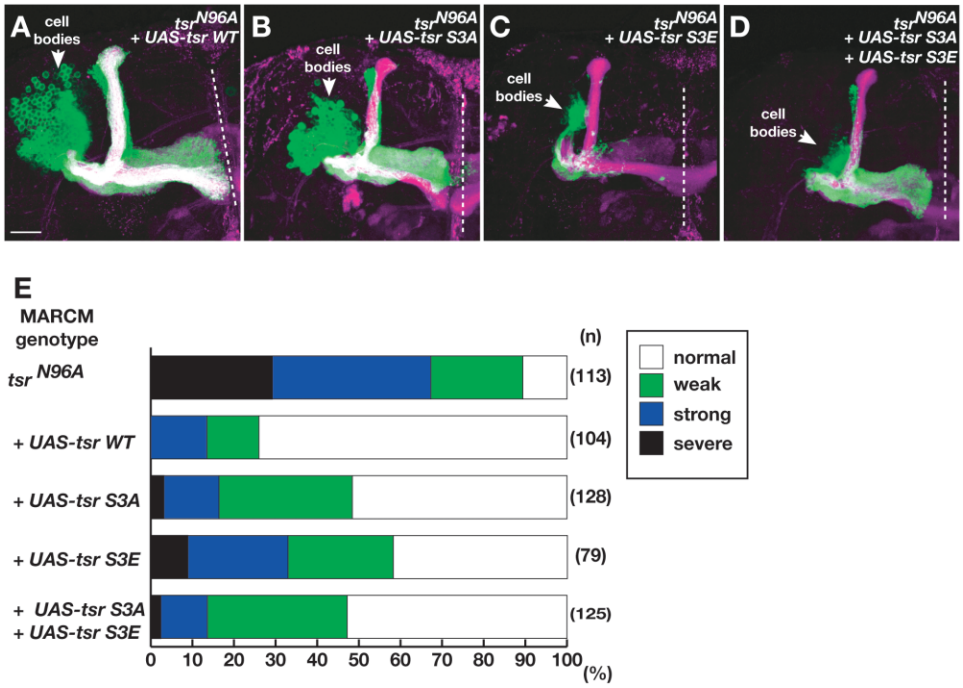

Figure 2. Regulation of Cell Proliferation and Axon Growth by Cofilin Phosphorylation

(A–D) Images of tsr^{N96A} MB neuroblast clones in the presence of transgenes overexpressing wild-type (WT) (A), S3A (B), S3E (C), or S3A + S3E cofilin (D), respectively. Scale bar, 20 μm.

(E) Quantification of transgene rescue of single-cell clones of tsr^{N96A} in the absence or presence of transgenes expressing either wild-type (WT) or serine 3 mutants of cofilin S3A, S3E, or S3A + S3E cofilin, respectively.

ability of various cofilin transgenes to rescue $tsr^{-/-}$ neuroblast proliferation defects. Overexpression of wild-type cofilin (*UAS-tsr WT*) in $tsr^{-/-}$ neuroblast clones fully restored cell proliferation, as these clones contain a full complement of all three classes of MB neurons (Figure 2A). Overexpression of S3A cofilin (*UAS-tsr S3A*) in $tsr^{-/-}$ clones partially rescued the cell proliferation phenotype, as only the two first-born classes of neurons (γ and α′β′, Figure 1A) were generated in these neuroblast clones (Figure 2B). This is consistent with the reduced neuronal numbers from these clones when compared to the wild-type rescue. Overexpression of S3E cofilin (*UAS-tsr S3E*) had no rescue effect on neuroblast proliferation, as the cell numbers in these neuroblast clones remained 15 to 30 (Figure 2C).

Using the same strategy, we examined single-cell clones of γ neurons to assay for axon growth. Overexpression of wild-type cofilin effectively rescued $tsr^{-/-}$ axon growth defects. Similar experiments using S3A or S3E cofilin also showed some rescue effects; however, neither of the transgenes rescued as effectively as wild-type cofilin, although S3A cofilin rescued better than S3E (Figure 2E).

These results suggest that cofilin phosphorylation regulates both cell proliferation and axon growth. In the case of cell proliferation, the nonphosphorylatable S3A cofilin has significant rescue activity, while the S3E is completely inactive, consistent with the findings of in vitro studies in which S3A provides constitutive depolymerization activity, while S3E has little or no actin depolymerization activity (Agnew et al., 1995; Abe et al., 1996). In the case of axon growth, however, both S3A and S3E have some rescuing effects on axon growth, suggesting that phosphorylated forms of cofilin might provide some function in axon growth. Indeed, a recent study showed that, while unphosphorylated cofilin promotes actin depolymerization, phosphorylated cofilin promotes actin polymerization (Ghosh et al., 2004). To test this model in vivo, we coexpressed both S3A and S3E cofilin in $tsr^{-/-}$ neurons. We found that coexpression of S3E and S3A cofilin did not rescue $tsr^{-/-}$ phenotypes to wild-type rescue levels for cell proliferation (Figure 2D, compared with Figure 2B) or axon growth (Figure 2E). This suggests that unphosphorylatable and phosphomimetic cofilins acting in *trans* cannot fully restore cofilin activity. Our experiments then suggest that cycling between phosphorylated and nonphosphorylated cofilin is essential for optimal cell proliferation and for axon growth and that S3E cofilin may have some residual actin depolymerization activity (as suggested by Agnew et al., 1995) to promote axon growth.

Essential Function of Cofilin Phosphatase Slingshot in Axon Growth

To examine how cofilin phosphorylation is regulated, we performed genetic studies on the cofilin phosphatase encoded by *ssh* (Niwa et al., 2002). Neuroblast clones homozygous for null alleles of *ssh* (ssh^{1-63} and ssh^{1-11}) did not have any obvious reduction of cell numbers (Figures 3C and 3D). Therefore, unlike cofilin, Ssh is not required for cell proliferation. However, all *ssh* neuroblast clones exhibited axon growth or growth and guid-

ance defects (Figure 3A). In "severe" cases (approximately 10%), *ssh*$^{-/-}$ axons failed to extend beyond the peduncle (blue open arrowhead in Figure 3B). Guidance defects were also detected either at the peduncle, where a large accumulation of axons led to the disorganization of the peduncle, or from the dendrite region (red arrows, Figure 3B). Approximately 90% of *ssh*$^{-/-}$ neuroblast clones exhibited only axon growth defects (Figure 3A), which were categorized as "strong" (Figure 3C) or "weak" (Figure 3D) (see Figure 3A for definitions). Developmental studies indicate that, at least for γ and α/β neurons, these defects are a direct result of axon extension failure (Supplemental Figure S1 [http://www.neuron.org/cgi/content/full/44/5/779/DC1/]).

We did not detect obvious axon growth defects in *ssh*$^{-/-}$ single-cell γ clones (data not shown). This is possibly because axon growth is more sensitive to *tsr* than to *ssh* mutations or because of perdurance effects (although homozygous mutant for the *ssh* mutation, clones may inherit enough wild-type protein or mRNA from heterozygous parental neural precursors to support Ssh function for some time after clone generation). To compare mutant phenotypes of *ssh* and *tsr* in axon growth, we also analyzed *ssh*$^{-/-}$ α/β-only neuroblast clones. The *ssh*$^{-/-}$ α/β axons displayed axon growth defects (Figure 3E, 3 out of 5 for *ssh*$^{1-11}$) similar to those observed in *tsr*$^{-/-}$ α/β clones (Figure 1M).

Dephosphorylating Cofilin Is the Major Function of Ssh in Axon Growth

Given the similarity of phenotypes between *ssh* and *tsr*, we next investigated whether Ssh regulates axon growth through cofilin dephosphorylation. We first tested whether Ssh phosphatase activity is required for axon growth. Overexpression of *UAS-ssh WT* or *UAS-ssh CS* (a point mutation in the phosphatase domain that renders it inactive; Niwa et al., 2002) in MB neurons did not result in gross axon defects (data not shown). Expression of *UAS-ssh WT*, but not *UAS-ssh CS*, in *ssh*$^{-/-}$ neuroblast clones rescued the *ssh* mutant defects (Figures 3F and 3G, quantified in Figure 3A), indicating that Ssh phosphatase activity in MB neurons is essential for axon growth.

We then performed transgenic suppression experiments by expressing different cofilin transgenes in *ssh*$^{-/-}$ clones. Strikingly, expression of S3A or wild-type cofilin in *ssh*$^{-/-}$ clones almost completely suppressed the *ssh*$^{-/-}$ defects (Figures 3H and 3I, quantified in Figure 3A). In contrast, expression of S3E cofilin produced a very weak effect (Figure 3A; data not shown). The suppression of the *ssh* phenotype by the overexpression of active cofilin indicates that the major function of Ssh in axon growth is to dephosphorylate cofilin.

To determine whether regulation of cofilin by Ssh is required for axon growth in other neurons, we also examined *ssh*$^{-/-}$ axon projections of contralateral projecting neurons of the optic lobe (OL) and the antennal lobe (AL) (Figure 3J). In both cases, we found highly penetrant axon growth phenotypes in *ssh*$^{-/-}$ neuroblast clones (Figures 3L and 3N, compared with Figures 3K and 3M; quantified in Figure 3O). These phenotypes were rescued by expressing wild-type, but not phosphatase inactive, Ssh in *ssh*$^{-/-}$ neuroblast clones (Figure 3O), indicating that Ssh regulates axon growth in these neurons cell-autonomously in a phosphatase-dependent manner. Furthermore, expression of active cofilin also suppressed these *ssh* growth defects (Figure 3O). Therefore, cofilin dephosphorylation by Ssh most likely plays a general role in axon growth of many neuronal types.

Overexpression of *Drosophila* LIM Kinase Disrupts Axon Growth

Previous biochemical studies have established cofilin as a direct target of LIM kinase. To determine if *Drosophila* LIMK1 is the cofilin kinase in MB neurons, we overexpressed LIMK1 in all MB neurons, which resulted in axon growth defects (Figures 4A–4C and 4E). In "severe" cases, all axon lobes were truncated. In addition, there were axon guidance defects at the peduncle, where axons formed a ball-like structure (Figure 4A). In cases of "strong" phenotypes, no guidance defects were detected, but both dorsal and medial axons were truncated (Figure 4B). In cases of "weak" phenotypes, axon growth defects were detected only in the dorsal lobes, while the medial lobes appeared normal (Figure 4C). The expression level of individual transgenic lines caused the variability in the extent of axon defects. As determined from the epitope tag (HA) staining (data not shown), stronger expression lines (lines M1 and M6) were associated with highly penetrant, severe axon growth and guidance defects, while weaker expression lines (F4 and M7) were associated with a mixture of severe, strong, weak, and, in some cases, no axon defects (Figure 4E). Overexpression of kinase-inactive forms of LIMK1 (*UAS-LIMK1 KI*) at comparable levels (as determined by anti-HA staining where LIMK1 KI is similarly localized to axons as wild-type LIMK1) resulted in normal axon projections (Figures 4D and 4E). This indicates that the axon growth defects caused by LIMK1 overexpression depend on its kinase activity.

Developmental studies indicate that the LIMK1 overexpression phenotype is similar to the *ssh*$^{-/-}$ phenotype. For at least γ and α/β neurons, these phenotypes are also a result of axon extension failure (Supplemental Figure S1 [http://www.neuron.org/cgi/content/full/44/5/779/DC1/]). To test whether endogenous LIMK1 plays a role in MB morphogenesis, we expressed LIMK1 RNAi in MB neurons. This resulted in axon guidance and some axon growth defects (Supplemental Figure S2). Therefore, LIMK1 is likely to play an endogenous role in MB morphogenesis.

Cofilin Phosphorylation Contributes to the LIMK1 Overexpression Phenotype

The similarities between the *ssh*$^{-/-}$ and LIMK1 overexpression phenotypes suggest that LIMK1 and Ssh exert their effects by regulating a common substrate, cofilin. To genetically test whether LIMK1 overexpression leads to the inactivation of cofilin through phosphorylation, we coexpressed either Ssh or cofilin in a LIMK1 overexpression background. We focused our experiments on the transgenic line *UAS-LIMK1 WT F4*, which has an intermediate level of expression, allowing sensitive genetic interactions to be detected (Figure 4E). Consistent with the idea that LIMK1 and Ssh regulate the phosphor-

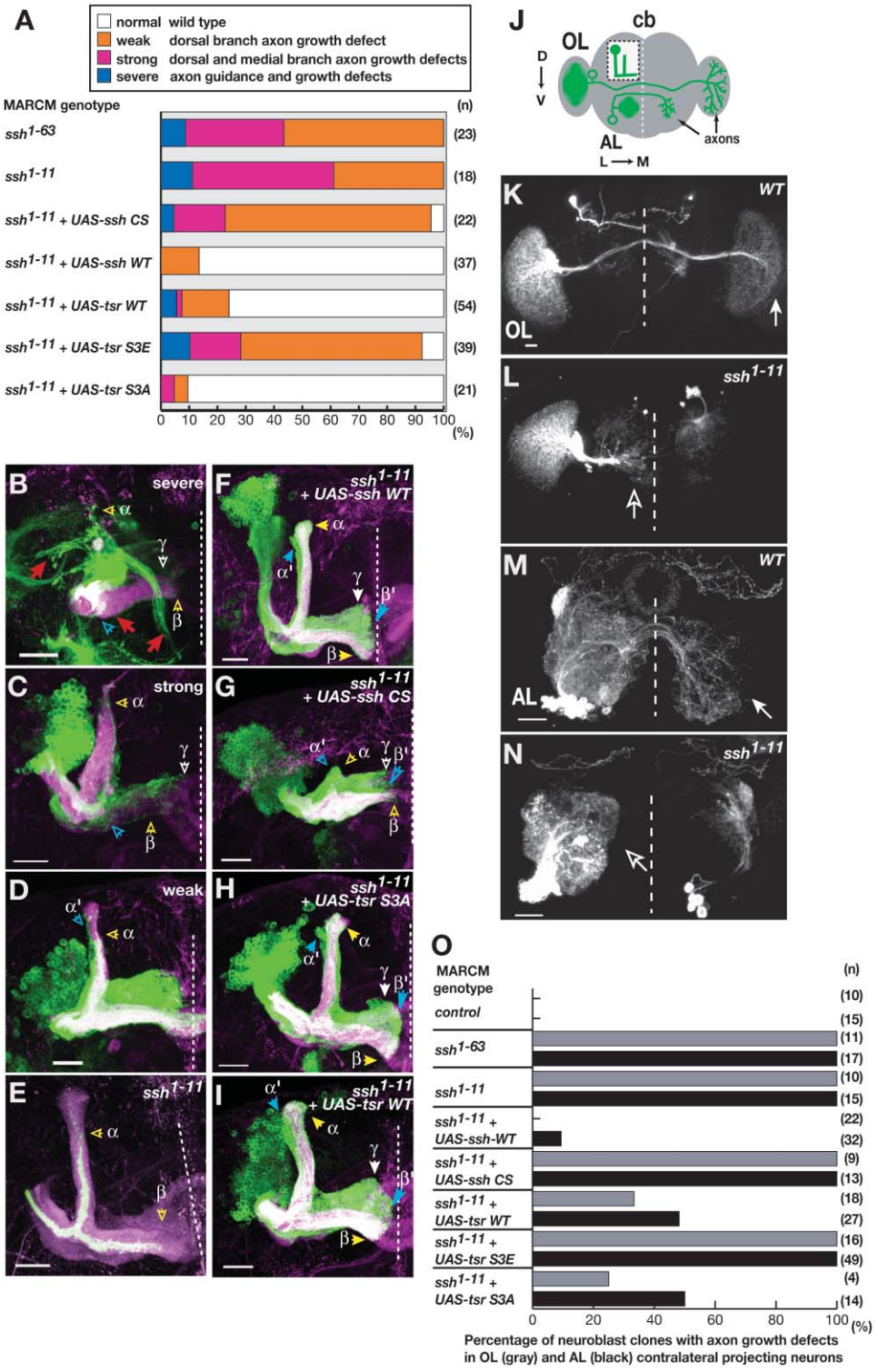

Figure 3. Function of Cofilin Phosphatase Slingshot in Axon Growth

(A) Quantification of *ssh*$^{-/-}$ axon growth and guidance defects in the absence or presence of transgenes expressing wild-type (WT) Ssh, phosphatase-inactive (CS) Ssh, wild-type cofilin, S3A or S3E cofilin. n, number of neuroblast clones examined. (B–D) Images of *ssh* neuroblast clones of either *ssh*$^{1-11}$ (B and D) or *ssh*$^{1-63}$ (C), representing severe (B), strong (C), or weak (D) phenotypes. Red arrows in (B) indicate axon guidance defects. (E) Image of *ssh*$^{1-11}$ neuroblast clone containing only α/β neurons, showing axon growth defects in dorsal and medial lobes. (F–I) Representative images of *ssh*$^{1-11}$ neuroblast clones expressing wild-type Ssh (F), phosphatase-inactive Ssh (CS) (G), S3A (H), or wild-type (I) cofilin. Filled or open arrowheads indicate normal or defective axon growth, respectively. In some images, MB cell bodies have been removed to avoid overlaps with the axonal lobes or wandering neurite projections after Z-projection. (J) Schematic of the *Drosophila* brain at the adult stage and the neurons used for morphological analyses. The boxed region shows the location of the MB neurons in the left hemisphere

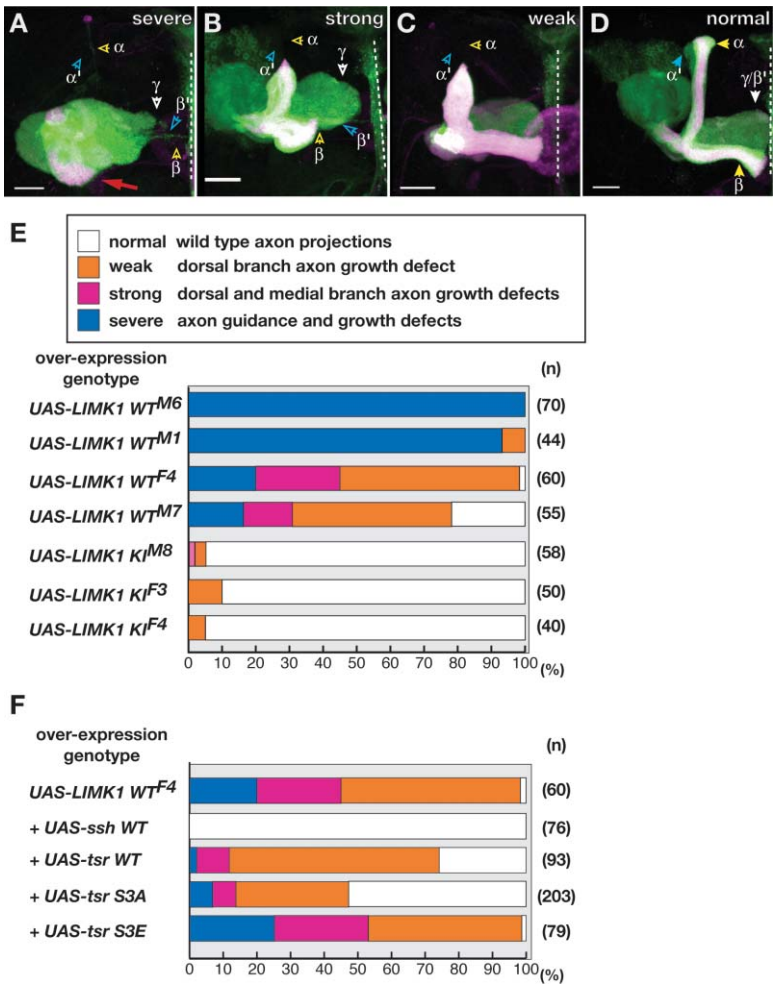

Figure 4. LIMK1 Regulates Axon Growth through Cofilin Phosphorylation

(A–D) Representative images of MB neurons overexpressing wild-type LIMK1 (A–C), representing severe, strong, and weak categories, or kinase-inactive LIMK1 (KI) (D), using the *Gal4-OK107* driver. Filled or open arrowheads indicate normal or defective axon growth, respectively. Scale bars, 20 μm. In these experiments, male offspring carrying LIMK1 transgenes were crossed to females carrying the following genotype: *yw*; FRT^{G13}, *UAS-mCD8::GFP*; +/+; *Gal4-OK 107*. Offspring flies carrying FRT^{G13}, *UAS-mCD8::GFP*; +/+; *Gal4-OK 107*/+ together with the one copy of the expression transgene were analyzed for phenotypes.

(E) Quantification of axon growth and guidance defects in LIMK1 overexpressing neurons, using different individual insertion lines of either WT or KI transgenes as indicated.

(F) Quantification of axon growth and guidance defects in LIMK1 overexpressing neurons, using the transgenic line *UAS-LIMK1* WT^{F4}, in the absence or presence of wild-type Ssh expression transgenes (*UAS-ssh*), wild-type or mutant cofilin expression transgenes (*UAS-tsr WT*, *S3A*, or *S3E*). n, number of brain hemispheres examined.

ylation of a common substrate, coexpression of wild-type Ssh fully suppressed the LIMK1 phenotype (Figure 4F). In addition, coexpression of either wild-type or S3A cofilin also suppressed the LIMK1 overexpression phenotype (Figure 4F). These experiments support the model that axon growth defects caused by LIMK1 overexpression are in large part a result of cofilin inactivation.

The Rho-Rok Signaling Pathway Positively Regulates *Drosophila* LIMK1 Function

So far, we have demonstrated that axon growth requires cofilin and that cofilin activity is regulated positively by Ssh phosphatase and negatively by LIM kinase (Figure 8). How is this cytoskeletal pathway directed by Rho GTPases in vivo?

We first examined the role of the Rho-Rok pathway in regulating LIMK. Since MB axon growth is sensitive to the level of LIMK1 activity, we performed genetic interaction studies, either reducing the gene dose of endogenous Rho signaling components by half (Figure 5A) or overexpressing components of the Rho pathway (Figure 5B) in a LIMK1 overexpression background. Removing one copy of *Rho1* (also called *RhoA*) strongly suppressed the axon growth phenotype caused by LIMK1 overexpression (Figure 5A). Halving the gene dose of the *Drosophila* Rho effector kinase *Rok* (also called *Drok*) also suppressed the LIMK1 overexpression phenotype (Figure 5A). However, this effect is much weaker, possibly because the Rok level is not as dose sensitive (Billuart et al., 2001). On the other hand, coex-

of the central brain (cb). Shown from the left hemisphere are the optic lobe (OL) contralateral projection neurons, which elaborate dendrites (green shading) ipsilaterally to one optic lobe but project axons contralaterally to the opposite optic lobe. Also shown from the left hemisphere are the antennal lobe (AL) contralateral projection neurons, which elaborate their dendrites (green shading) ipsilaterally to one antennal lobe but project axons contralaterally to the opposite antennal lobe. (K–N) Representative images of neuroblast clones of either *wild-type* (K and M) or ssh^{1-11} (L and N), OL (K and L), or AL (M and N) contralateral projecting neurons. White arrows (K and M) indicate wild-type axon termination points. Open white arrowheads indicate axon growth defects in ssh^{1-11} neuroblast clones, none of which cross the midline. (O) Quantification of axon growth defects in OL and AL contralateral projection neurons for wild-type or *ssh* neuroblast clones in the absence or presence of wild-type (WT) or phosphatase-inactive (CS) Ssh expressing transgenes or transgenes expressing wild-type, S3A or S3E cofilins, as indicated. n, number of neuroblast clones examined. Scale bars, 20 μm.

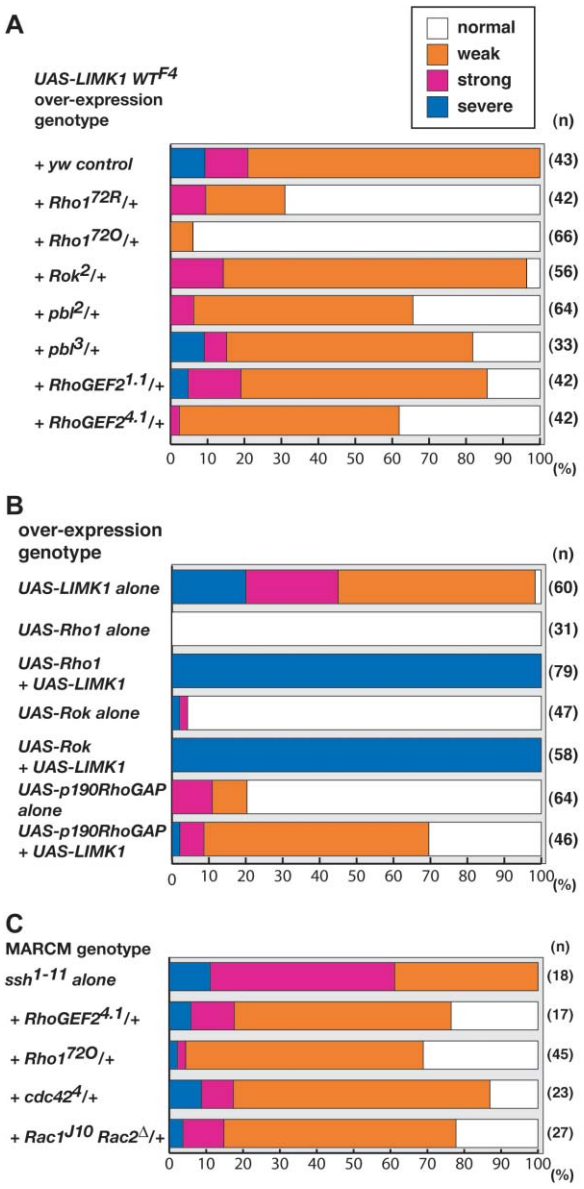

Figure 5. The Rho1 Signaling Pathway Positively Regulates *Drosophila* LIMK1

(A) Quantification of axon growth defects in LIMK1 overexpressing neurons in the absence or presence of one mutant copy of Rho1 signaling components as indicated. To minimize variations in genetic background, *yw* (control) or Rho1 pathway mutants were tested by crossing female mutants to the males carrying the following genotype: *hs-FLP*, *UAS-mCD8::GFP/Y*; +/+; *UAS-LIMK1 WT^{F4}/Tm3,Sb^{1}*; *Gal4-OK 107/+*. Female offspring carrying the genotype *hs-FLP*, *UAS-mCD8::GFP/+*; *UAS-LIMK1 WT^{F4}/+*; *Gal4-OK 107/+* together with the loss of one copy of the Rho1 signaling gene were used for phenotypic analysis. (B) Quantification of axon growth defects in LIMK1 overexpressing in the absence or presence of transgenes expressing Rho1 pathway components as indicated. All additional trangenes were first recombined to *UAS-LIMK1 WT^{F4}*. Male offspring were then crossed to females carrying the following genotype: *yw*; *FRT^{G13}*, *UAS-mCD8::GFP*; +/+; *Gal4-OK 107*. Offspring carrying the *FRT^{G13}*, *UAS-mCD8::GFP*; *UAS-LIMK1 WT^{F4}/+*; *Gal4-OK 107/+* together with the one copy of the additional transgene were used for phenotypic analysis. (C) Quantification of axon growth and guidance defects of *ssh* neuroblast clones in the absence or presence of one mutant copy of *Rho1*, *RhoGEF2*, *Cdc42*, or *Rac* (*Rac1* and *Rac2*), as indicated. n, number of brain hemispheres (A and B) or neuroblast clones (C) examined.

pressing Rok or Rho1 with LIMK1 strongly enhanced the axon growth defects, even though overexpressing either Rho1 or Rok alone did not disrupt axon growth (Figure 5B). These results suggest that Rho1 and Rok positively regulate LIMK1 activity.

We also tested the possible involvement of upstream regulators of Rho1. Introducing one mutant copy of *RhoGEF2* (Barrett et al., 1997) or *pebble* (*pbl*) (Prokopenko et al., 1999), two guanine nucleotide exchange factors known to positively regulate Rho1 or overexpression of the Rho1 inhibitor p190 RhoGAP (Billuart et al., 2001) all resulted in suppressing the LIMK1 overexpression phenotype (Figures 5A and 5B, respectively). Taken together with known biochemical activities of these signaling components, our genetic interaction data suggest that Rho1 activates Rok, which then directly activates LIMK1. In turn, this pathway is likely to be regulated positively by at least two RhoGEFs (RhoGEF2 and Pbl) and negatively by p190 RhoGAP in MB neurons in vivo (Figure 8).

While LIMK1 overexpression in MB neurons provides a sensitive assay for genetic interactions, we also tested our model using endogenous components. According to the model, overexpression of LIMK1 results in cofilin hyperphosphorylation, which is phenocopied in *ssh* mutants. Therefore, modulating the level of Rho1 signaling should also modify the *ssh$^{-/-}$* phenotype in a similar manner. Indeed, we found that loss of one copy of either *Rho1* or *RhoGEF2* also markedly suppressed the *ssh$^{-/-}$* defects (Figure 5C).

The Cdc42/Rac/Pak Pathway Positively Regulates LIMK1

Biochemical studies have shown that LIM kinase is activated by Pak, a downstream effector kinase for Rac and Cdc42. We next tested whether Pak activation could affect the LIMK pathway in axon growth. In similar genetic interaction experiments, we found that introducing three independently generated *Drosophila Pak* mutant alleles suppressed the LIMK1 overexpression phenotype (Figure 6A). In addition, Pak overexpression also resulted in axon growth and guidance defects similar to those seen with LIMK1 overexpression (Figure 6B; Supplemental Figure S3 [http://www.neuron.org/cgi/content/full/44/5/779/DC1/]), consistent with the model in which Pak activates LIMK1, leading to cofilin hyperphosphorylation (Figure 8). As predicted from this model, coexpression of active versions of cofilin with Pak resulted in a partial suppression of the growth and guidance defects (Figure 6B).

We next determined which Rho GTPase pathway (*Cdc42*, *Rac1/Rac2*, or *Rho1*) regulates *Drosophila* Pak. We found that loss of one copy of *Cdc42* resulted in a strong suppression of the *Pak* overexpression phenotypes. Similar reduction of *Rac1* and *Rac2* (*Rac1^{J10}*, *Rac2$^{\Delta}$*) resulted in weaker suppression. In contrast, reducing *Rho1* resulted in a slight enhancement of the Pak over-

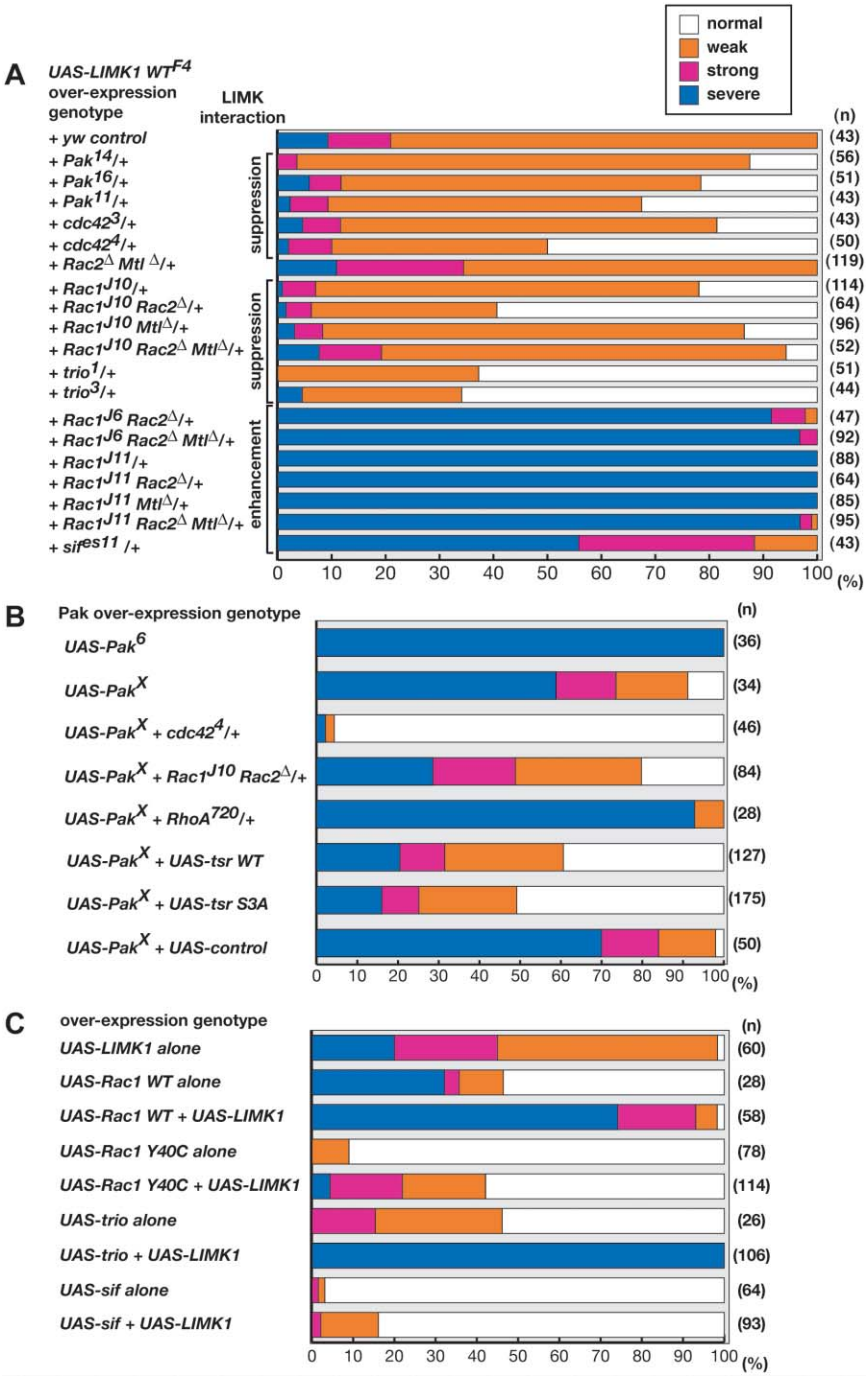

Figure 6. Genetic Interactions between the Rac/Cdc42/Pak and the LIMK1 Pathways

(A) Quantification of axon growth and guidance defects in LIMK1 overexpressing neurons in the absence or presence of one mutant copy of *Pak*; *Cdc42*; the *Rac* GTPases *Rac1*, *Rac2*, and *Mtl*; or Rac GEFs *trio* and *sif*, as indicated. Genetic crosses were performed as described in Figure 5A. n, number of brain hemispheres examined.

(B) Quantification of axon growth and guidance defects in *Pak* overexpressing neurons in the absence or presence of one mutant copy of *Cdc42* or *Rac*, or cofilin expressing transgenes. In coexpression experiments, each transgene to be tested was first recombined to *UAS-Pak WT^{X}*. Male offspring carrying both transgenes were then crossed to females carrying the following genotype: *yw; FRT^{G13}*, *UAS-mCD8::GFP*; +/+; *Gal4-OK 107*. Offspring carrying *UAS-Pak WT ^{X}* /+; *FRT^{G13}*, *UAS-mCD8::GFP*; +/+; *Gal4-OK 107*/+ together with the one copy of the expression transgene were analyzed for phenotypes. To test for any possible Gal4 titration effects, we used an additional copy of *UAS-mCD8::GFP* as a control.

(C) Quantification of axon growth defects in LIMK1 overexpressing neurons, using the transgenic line *UAS-LIMK1 WT^{F4}* alone or in combination with additional UAS-transgenes, as indicated.

expression phenotype (Figure 6B). This suggests that the Pak overexpression phenotype specifically reflects the positive signaling input from Cdc42 and Rac in vivo.

We next tested whether mutations in the *Cdc42* or *Rac* genes (*Rac1*, *Rac2*, *Mtl*, and the different combinations) would modify the LIMK1 overexpression phenotype. Reducing the *Cdc42* activity led to the suppression of the LIMK1 phenotype (Figure 6A), suggesting that Cdc42 acts through Pak to activate LIMK1. Loss of one copy of both Rac2 and Mtl did not alter the LIMK1 phenotype. However, the LIMK1 phenotype is very sensitive to the levels of endogenous *Rac1*, as introducing one copy of a strong hypomorphic allele of *Rac1* (*Rac1*^{J10}) significantly suppressed the LIMK1 phenotype. This suppression was further enhanced when one copy of a null allele of *Rac2* was introduced (Figure 6A). These results suggest that Rac signaling (in particular, Rac1 and Rac2) also acts to activate LIMK1. This suggestion was also supported by the overexpression experiment. Overexpression of wild-type Rac1 (*UAS-Rac1 WT*) resulted in a weak LIMK1-like phenotype. However, when Rac1 and LIMK1 were coexpressed, axon growth defects were enhanced (Figure 6C). Together with previous biochemical studies, these results suggest that Cdc42 and Rac act via Pak to activate LIMK1 (Figure 8).

To verify these genetic interactions with endogenous components, we investigated whether reducing either Cdc42 or Rac activity would modify the *ssh*$^{-/-}$ phenotype. As with Rho1, reducing Cdc42 or Rac activity also partially suppressed the *ssh*$^{-/-}$ defects (Figure 5C). Thus, our data indicate that Rho1, Cdc42, and Rac can all act through distinct downstream kinases to activate LIMK1 (Figure 8).

Rac Also Signals through a Pak-Independent Pathway to Antagonize the LIMK Pathway

Surprisingly, reducing Rac GTPase activity can also result in enhancing the LIMK1 overexpression phenotype (Figure 6A). For instance, the suppression effect of *Rac1*^{J10} *Rac2*$^{\Delta}$/+ was reverted by heterozygosity of *Mtl* (*Rac1*^{J10} *Rac2*$^{\Delta}$ *Mtl*$^{\Delta}$/+). This enhancement is more evident when one copy of the strongest allele of Rac1 was introduced into the LIMK1 overexpression background (*Rac1*^{J11}/+). This effect was not due to dominant effects of this *Rac1* allele, as in the same genetic background *Rac1*^{J11}/+ animals did not display LIMK1-like growth defects without the LIMK1 expression transgene. Introduction of another hypomorphic allele of *Rac1* (*Rac1*^{J6}) together with *Rac2* (*Rac1*^{J6} *Rac2*$^{\Delta}$/+) also strongly enhanced the LIMK1 overexpression phenotype (Figure 6A).

One interpretation of these results is that, while Rac can activate LIMK1 (via Pak), there is an alternative pathway downstream of Rac, acting antagonistically to LIMK1, that promotes axon growth. This is consistent with our previous finding that loss of Rac GTPase activity leads to axon growth defects in MB neurons (Ng et al., 2002). This pathway is likely to be Pak independent, as the Rac axon growth-promoting activity does not require direct binding to Pak (Ng et al., 2002), and Pak activation leads to axon growth inhibition (Figure 6B). To further verify the existence of a Pak-independent pathway in regulating axon growth, we made use of a well-described Rac1 effector domain mutant. In mammalian fibroblasts, Rac1 activates Pak1 and, through an independent downstream pathway, promotes lamellipodia formation. A Y40C mutation in the effector binding domain of Rac1 results in the loss of Pak1 activation, but the lamellipodia promoting activity is maintained (Joneson et al., 1996; Lamarche et al., 1996). Transgenic overexpression of Rac1 Y40C alone at levels comparable to those of wild-type Rac (data not shown) did not result in gross axon phenotypes (Figure 6C). However, in contrast to wild-type Rac1 that strongly enhanced LIMK1, coexpression of Rac1 Y40C strongly suppressed the LIMK1 overexpression phenotypes (Figure 6C). These results suggest that Rac1 activates a Pak-independent pathway to counteract the effects of LIMK1 activity on axon growth (Figure 8).

Different RacGEFs Couple to Different Axon Growth Pathways

We further tested whether upstream activators of Rac, RacGEFs, could regulate these distinct axon growth pathways. Trio encodes a RacGEF essential for axon guidance in MB neurons (Awasaki et al., 2000). We found that introducing one mutant copy of a *trio* significantly suppressed the LIMK1 overexpression phenotype (Figure 6A), suggesting that Trio acts to activate LIMK1. This was further verified by the overexpression experiments in which overexpression of wild-type Trio (UAS-*trio*) alone resulted in a mild LIMK1-like phenotype, while coexpression with LIMK1 resulted in a strong enhancement of the axon growth defects (Figure 6C). Trio has two GEF domains—GEF1 is specific for Rac1, Rac2, and Mtl in vitro and in vivo, and GEF2 can activate Rho1/RhoA in vitro (Bellanger et al., 1998; Newsome et al., 2000). Overexpression of the isolated Trio GEF1 domain (UAS-*trio GEF1*) in MB neurons resulted in severe axon growth defects, whereas overexpression of the isolated Trio GEF2 domain (UAS-*trio GEF2*) did not result in any gross defects (data not shown). These results support the model that, in MB neurons, Trio, via its GEF1 domain, acts through Rac and Pak to activate LIMK1 (Figure 8). These findings are also consistent with those of previous studies in which Trio acted via Rac/Pak to regulate *Drosophila* photoreceptor axon guidance (Newsome et al., 2000).

In contrast to Trio, loss of one copy of *still life* (*sif*), encoding a different RacGEF (Sone et al., 1997, 2000), markedly enhanced the LIMK1 phenotype (Figure 6A). In overexpression experiments, *UAS-sif* alone did not result in gross axon defects. However, coexpression of Sif resulted in a strong suppression of the LIMK1 phenotype (Figure 6C). These experiments suggest that Sif activates the pathway that acts antagonistically to LIMK1 (Figure 8).

Lack of Evidence that the Rac-Mediated Axon Growth-Promoting Pathway Acts through Actin Polymerization

Our data suggest that Rac promotes axon growth via a pathway antagonistic to Pak and LIMK1. How does this pathway ("X" in Figure 8) act to promote axon growth? One strong possibility is that Rac stimulates actin polymerization to promote axon growth. We therefore tested

a number of candidate genes known to promote actin polymerization. We established the following genetic criteria by which these candidate pathways should work. First, like Rac, loss of the candidate gene should result in axon growth defects. Second, genetic interactions with LIMK1, either through loss- or gain-of-function analyses, should show that they act antagonistically to LIMK1.

We first tested the role of the actin nucleation factor SCAR-Arp2/3 complex. Rac has been shown to promote de novo actin polymerization through interactions via SCAR and the Arp2/3 complex (Eden et al., 2002). Activation of the SCAR-Arp2/3 complex is required to establish cell protrusions during lamellipodia and filopodia formation, making it a good candidate pathway for promoting axon growth. We tested this hypothesis by making MARCM clones in MB neurons using null alleles of *SCAR*, *WASp* (a protein related to SCAR, also called *Wsp*), double mutants for *SCAR* and *WASp*, or *Arpc1* (Flybase-*Sop2*), an essential component of the Arp2/3 complex. We did not detect axon growth defects in single-cell (Figures 7A–7D) or neuroblast clones (data not shown). In addition, reduction of *SCAR* or *Sop2* levels did not modify the LIMK1 overexpression phenotype (Figure 7H). Furthermore, overexpression of SCAR did not suppress, but mildly enhanced, the LIMK1 overexpression phenotype (Figure 7I). Taken together, these results suggest that the SCAR/WASp-Arp2/3 pathway does not play an essential role in axon growth of MB neurons, and it is unlikely that this pathway contributes to the Rac pathway that promotes axon growth.

We also tested several other known regulators of actin polymerization for their contribution to MB axon growth. The actin polymerization stimulators profilin (encoded by *chickadee* or *chic*) and Enabled (Ena) have been shown to be essential for axon growth and guidance in *Drosophila* (Wills et al., 1999a, 1999b). In addition, genetic interaction studies suggest that these proteins may be involved in Rac GTPase signaling (Liebl et al., 2000; Fritz and VanBerkum, 2002). When assayed for MB axon growth, both $ena^{-/-}$ and $chic^{-/-}$ single-cell (Figures 7E and 7F, quantified in Figure 7A) and neuroblast clones (data not shown) exhibited drastic axon growth defects. Interestingly, when examined at higher resolutions, neither *ena* nor *chic* axons displayed filopodia- and lamellipodia-like protrusions at the axon termini (data not shown) characteristic of $tsr^{-/-}$ neurons (Figure 1K). Our genetic interaction experiments found no evidence that *ena* or *chic* act antagonistically to LIMK1. In fact, Ena overexpression strongly enhanced the LIMK1 overexpression phenotype (Figures 7H and 7 I). Thus, although both Ena and profilin are essential for MB axon growth (Figure 8), they do not appear to constitute the Rac-mediated axon growth-promoting pathway.

Finally, we also tested the Formin-class protein Diaphanous (Dia), as it has been implicated in regulating actin polymerization downstream of Rho GTPases. $dia^{-/-}$ MB neurons do not exhibit axon growth defects in single-cell clones (Figures 7G and 7A) or in neuroblast clones, which exhibit strong cell proliferation defects (data not shown). Interestingly, reducing Dia activity appears to suppress the LIMK1 overexpression phenotype (Figure 7H), suggesting that Dia can act in a pathway that enhances, but does not antagonize, LIMK1.

Discussion

Using *Drosophila* mushroom body neurons as a genetic model, we have characterized several signaling pathways through which Rho GTPases regulate axon growth in vivo (Figure 8). We discuss here new insights obtained from these genetic analyses.

Cofilin Is Essential for Axon Growth

Actin polymerization at the leading edge is generally thought to provide the driving force for membrane protrusions such as lamellar extension in migrating cells (Svitkina and Borisy, 1999; Pollard et al., 2000) or filopodia and lamellipodia extensions for neuronal growth cone advance (e.g., Forscher and Smith, 1988; Mallavarapu and Mitchison, 1999). Here we demonstrate that cofilin is essential for axon growth in vivo. Since cofilin has both pointed-end depolymerization activity and F-actin severing activity, there are at least two possible explanations, on the basis of biochemical and cell biological studies in other cell types, for its essential role in axon growth (e.g., Carlier et al., 1997; Svitkina and Borisy, 1999; Dawe et al., 2003; Ghosh et al., 2004). First, actin polymerization at the leading edge requires a constant supply of monomeric actin subunits derived from depolymerization at the pointed end. Second, the severing activity of cofilin allows generation of free barbed ends as templates for actin polymerization. While we have not ruled out the contributions of either of the above processes to axon growth, we find that loss of cofilin does not simply result in a lack of filopodia or lamellipodia. Instead, the overabundance of filopodia- and lamellipodia-like structures retained in cofilin mutant axons suggests a third possibility: growth cone advance is inhibited when filopodia/lamellipodia cannot be disassembled upon the loss of cofilin activity.

LIM Kinase and Ssh Phosphatase Are Key Regulators of Cofilin in Axon Growth

How is cofilin activity regulated during axon growth? A number of recent studies have addressed the role of cofilin phosphorylation by LIM-kinase and Ssh phosphatase in cultured neurons. For example, overexpression of active forms of cofilin in rat cortical neurons results in an increase in both the number of filopodia and the degree of neurite extension (Meberg and Bamburg, 2000). Overexpression of active forms of LIMK in chick dorsal root ganglion neurons represses growth cone motility and neurite extension. The LIMK effects are likely to be mediated through cofilin, as cotransfection of either mammalian Ssh or the S3A form of cofilin suppresses the LIMK effects (Endo et al., 2003). Cofilin phosphorylation by LIMK is further implicated in semaphorin-mediated growth cone collapse (Aizawa et al., 2001).

Our in vivo study confirms and extends these in vitro studies in several ways. First, using a transgenic rescue assay, we showed that neither phosphomimetic (S3E) nor nonphosphorylatable (S3A) cofilin or their combination can replace endogenous cofilin function. This suggests that cycles of cofilin phosphorylation ("inactivation") and dephosphorylation ("reactivation") are important during actin turnover to promote axon growth

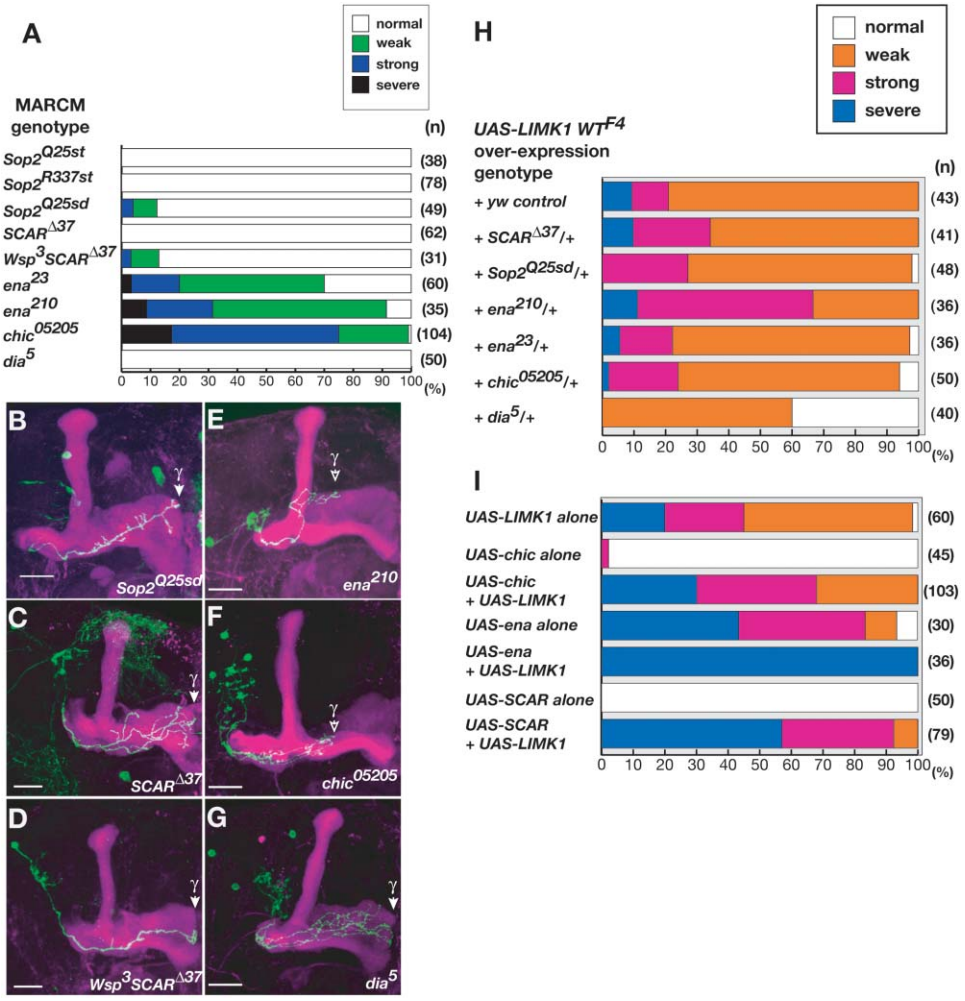

Figure 7. Phenotypic and Genetic Interaction Studies of Major Actin Polymerization Regulators

(A) Quantification of axon growth defects of single-cell clones of γ neurons mutant for *Sop2*, *SCAR*, *Wsp* + *SCAR*, *ena*, *chic*, or *dia*, as indicated. n, number of single-cell clones examined.

(B–G) Representative images of single-cell clones of γ neurons mutant for *Sop2*, *SCAR*, *Wsp* + *SCAR*, *ena*, *chic*, or *dia*, as indicated. Filled or open arrowheads indicate normal or defective axon growth, respectively. Scale bars, 20 μm.

(H and I) Quantification of axon growth defects in LIMK1 overexpressing neurons, in the absence or presence of one mutant copy of candidate genes (H) or in the absence or presence of overexpression transgenes (I).

To minimize variations in genetic background, these experiments were performed similarly to those depicted in Figures 5A and 5B. n, number of brain hemispheres examined.

(Figure 8) and that in vivo the factors that regulate cofilin phosphorylation must act in a delicate balance to optimize axon growth during development. Second, we showed that loss of Ssh also results in axon growth defects, and these defects can be suppressed by the expression of active cofilin, demonstrating that the major function of Ssh in regulating axon growth is cofilin dephosphorylation. Third, we showed that LIMK overexpression results in axon growth defects analogous to *ssh*, and this phenotype can be suppressed by the coexpression of Ssh or active cofilin. Taken together with existing biochemical data, these results firmly establish that regulation of cofilin phosphorylation by Ssh phosphatase and LIMK plays a pivotal role in regulating axon growth in vivo.

Although cofilin phosphorylation is essential for neuroblast proliferation, neither LIMK nor Ssh appears to be a key regulator. We did not detect cell proliferation defects in $ssh^{-/-}$ neuroblast clones or in LIMK1-overexpressing neurons, in contrast to $tsr^{-/-}$ clones. It is unlikely that cell proliferation is less sensitive to the reduction of cofilin activity than is axon growth. On the contrary, neuroblast clones homozygous for a hypomorphic allele of *tsr* (tsr^{1}) have strong defects in cell proliferation, but no defects in axon growth (data not shown). Taken together, these data suggest that cofilin phosphorylation during cell proliferation is regulated by a set of kinases/phosphatases different from those that regulate axon growth.

Convergent and Divergent Pathways Downstream of Rho GTPases

Our genetic analyses showed that Rho, Cdc42, and Rac all contribute to activation of the LIMK1 pathway, which

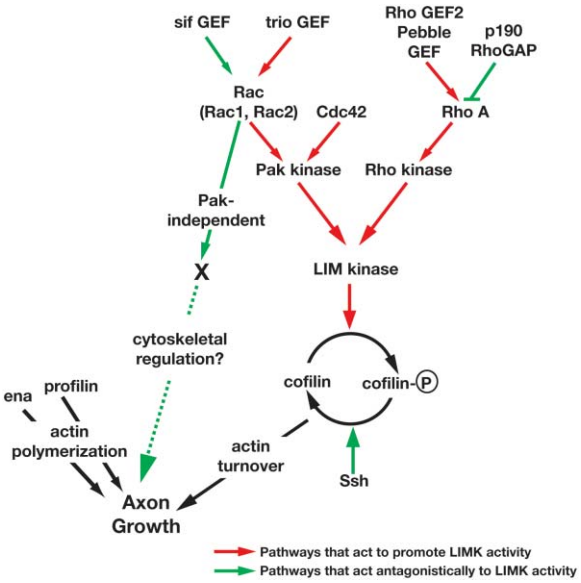

Figure 8. A Model of Signaling Pathways that Regulate Axon Growth

This model is derived from previous biochemical studies and genetic data from this study. See text for details.

leads to axon growth inhibition (Figure 8). However, previous cell biological data in vitro (Kozma et al., 1997) and loss-of-function mutant analysis in vivo (Lundquist et al., 2001; Hakeda-Suzuki et al., 2002; Ng et al., 2002) indicated that Rac GTPases act to promote axon growth. How can one resolve these seemingly opposite effects of Rac GTPases?

We provide several lines of evidence that, in addition to activating LIMK1, Rac GTPases also act via a second pathway to promote axon growth. First, reduction of Rac GTPase activity can also enhance the LIMK1 overexpression phenotype, suggesting that Rac could act antagonistically to LIMK1 to promote axon growth. Second, overexpressing Rac1 Y40C (a mutant with diminished binding to Pak) strongly suppresses the LIMK1 overexpression phenotype. Since Pak activation leads to axon growth inhibition and *Pak*$^{-/-}$ neuroblast clones do not have axon growth defects (data now shown), these data together suggest that the Rac pathway that counteracts the LIMK pathway is Pak independent, which is consistent with our previous studies in which transgenically supplied Rac1 Y40C rescued axon growth in the absence of all endogenous Rac (Ng et al., 2002). Third, we showed that two different RacGEFs can either enhance or suppress the LIMK pathway. This again suggests that different Rac signaling pathways act antagonistically to regulate axon growth.

Given the presence of these two pathways, it is likely that, depending on the signaling context, Rac can either inhibit or promote axon growth. Indeed, Rac activation has been shown to either promote or inhibit axon growth in different systems (reviewed in Luo, 2000). In addition, both attractive and repulsive axon guidance cues can signal through Rac GTPases to mediate these opposite effects in vivo (Fan et al., 2003; Gitai et al., 2003). We propose that one possible explanation for the above phenomena is that different cues selectively favor either the Pak/LIMK/cofilin phosphorylation pathway or the alternative axon growth-promoting pathway, resulting in different developmental outcomes. Our finding that two RacGEFs have opposite effects in modifying LIMK activity suggests that the selection of these pathways could be achieved by selectively engaging different GEFs. How RacGEFs selectively couple to different downstream effector pathways remains to be determined by future experiments.

Rac activation stimulates actin polymerization and leads to cell protrusions via lamellipodia formation (Machesky and Hall, 1997). However, our testing of several major classes of actin polymerization stimulators did not provide evidence that Rac promotes axon growth through the actin polymerization pathway. For instance, the SCAR-Arp2/3 pathway essential for de novo actin polymerization does not appear to contribute to MB axon growth in vivo. This is consistent with a recent study suggesting that the Arp2/3 pathway is also not essential for axon growth in cultured neurons (Strasser et al., 2004). Although the anticapping protein Enabled is essential for MB axon growth, genetic interaction data argue against its participation in the axon growth-promoting pathway downstream of Rac. This is also consistent with previous genetic analysis in *C. elegans*, indicating that Rac (Ced-10) and Ena (Unc-34) act in parallel pathways downstream of the netrin receptor (Gitai et al., 2003) to promote axon growth. Another possibility for the axon growth-promoting pathway is that Rac counteracts the LIMK pathway by activating Ssh. Recent in vitro data suggest that Rac can act to dephosphorylate cofilin (Nagata-Ohashi et al., 2004), thereby promoting actin turnover. However, we believe that the Rac-dependent axon growth pathway is unlikely to be via Ssh alone, given that, in the absence of *ssh*, Rac Y40C overexpression can still suppress the *ssh* growth phenotype (data not shown). Since axon growth also requires the regulation of microtubule dynamics and vesicle trafficking, both of which are thought to be Rho GTPase dependent (Etienne-Manneville and Hall, 2002), we propose that the Rac-mediated axon growth-promoting pathway may involve these processes.

In summary, our genetic analyses have begun to tease apart the complex signaling networks between Rho GTPases and the actin cytoskeleton in the context of axon growth in vivo. We have shown that Rho GTPases act through convergent and divergent signaling pathways to regulate axon growth. In addition to cofilin regulation, analyses of other actin polymerization regulators in MB neurons have established the relationship between these signaling pathways and the regulation of axon growth. The pathways identified here provide a foundation for future investigations as to how extracellular cues direct growth cone signaling to precisely wire neural circuits in vivo.

Experimental Procedures

Drosophila Strains

tsr mutant strains were gifts from M. Goldberg (Cornell University) (Chen et al., 2001). *tsr*^{N96A} and *tsr*^{N121} are both null alleles derived from P-element-mediated imprecise excision of the *tsr* locus. *ssh* mutants and transgenic Ssh or LIMK1 were described in Niwa et al., 2002. *Rac, Rho*, and *Cdc42* mutants and UAS transgenic strains

were as previously described (Ng et al., 2002; Strutt et al., 1997; Fehon et al., 1997). The following additional strains were also used in our study: *Rok*^{2} (Winter et al., 2001); *UAS-Rok* (Mizuno et al., 2002); *RhoGEF*$^{1.1}$ and *RhoGEF*$^{4.1}$ (Barrett et al., 1997); *pbl*^{2} and *pbl*^{3} (Prokopenko et al., 1999); *UAS-p190RhoGAP* (Billuart et al., 2001); *pak*^{11}, *pak*^{14}, *pak*^{16} (Hing et al., 1999; Newsome et al., 2000), and *UAS-pak* (Fan et al., 2003); *trio*^{1}, *trio*^{3}, and *UAS-trio* (Newsome et al., 2000); *sif*^{ES11} and *UAS-sif* (Sone et al., 2000); *Sop2*^{R337}, *Sop2*^{Q25sd}, and *Sop2*^{Q25st} (Hudson and Cooley, 2002); *Wsp*^{3}, *SCAR*^{D37}, and *UAS-SCAR* (Zallen et al., 2002); *ena*^{23}, *ena*^{210}, and *UAS-ena* (Ahern-Djamali et al., 1998); *chic*^{05205} and *UAS-chic* (Wills et al., 1999a; and gift from L. Cooley). *Drosophila* strains for MARCM analysis have been previously described (Lee et al., 1999; Ng et al., 2002), and standard recombination techniques were used to generate mutant strains. Flybase nomenclature is used for all *Drosophila* genes throughout the paper.

Molecular Biology

To generate *UAS-tsr WT* transgenic strains, the entire *tsr* ORF was subcloned into the pUAST transformation vector (Brand and Perrimon, 1993). Serine 3 site-specific mutant strains were constructed via site-directed mutagenesis and also subcloned into pUAST for germline transformation. To generate *UAS-DLIMK IR* transgenic lines, a cDNA product corresponding to the N-terminal kinase domain from a *Drosophila LIMK1* ORF was PCR amplified. This region corresponded to a nonredundant sequence (as determined by the BLASTN program) in the *Drosophila* genome (and therefore is likely to be specific to LIMK1 inhibition). The cDNA product was then subcloned "back-to-back," to create an inverse repeat, into a transformation vector that contains ten copies of the UAS target sequence (a gift from B. Dickson).

MARCM and Gal4-UAS Expression Studies

All flies were reared at 25°C, except in RNAi experiments, for which flies were raised at 29°C. Neuroblast and single-cell MARCM clones were generated by heat shock-induced FLP expression in newly hatched larvae or during puparium formation, when neuroblast proliferation is largely limited to MB neuroblasts, as previously described (Ng et al., 2002). In this study, all MB neurons and antennal lobe (AL) or optic lobe (OL) contralateral projecting neurons were visualized using the OK107 Gal4 driver expressing *UAS-mCD8::GFP*. Overexpression studies were also performed using the OK107 Gal4 driver, together with one copy of CD8::GFP (unless stated otherwise). For MARCM analyses, *Drosophila* brains were visualized by immunostaining with anti-CD8 and anti-FasII antibodies. In overexpression studies, neurons were visualized using the epifluorescent CD8::GFP marker together with anti-FasII staining. In almost all cases, two to three independently isolated transgenic lines were used in overexpression and transgenic rescue studies. Given the similarity in the effect of these transgenes, the quantified data reflect the pooled number of hemispheres or clones analyzed. All *Drosophila* brains were dissected, fixed, stained, and imaged as previously described (Ng et al., 2002).

Acknowledgments

We especially thank T. Uemura and M. Goldberg for reagents and advice during the initial stages of these experiments. We also thank G. Bashaw, B. Baum, L. Cooley, B. Dickson, C. Hama, Y. Nishida, R. Saint, E. Schejter, and the Bloomington *Drosophila* Stock Center for additional fly strains; and M. Simon, T. Meyer, L. Ma, and members of the Luo Lab for comments on the manuscript. Supported by NIH grant (R01-NS 36632) to L.L.

Received: May 3, 2004
Revised: August 20, 2004
Accepted: October 15, 2004
Published: December 1, 2004

References

Abe, H., Obinata, T., Minamide, L.S., and Bamburg, J.R. (1996). Xenopus laevis actin-depolymerizing factor cofilin: A phosphorylation-regulated protein essential for development. J. Cell Biol. *132*, 871–885.

Agnew, B.J., Minamide, L.S., and Bamburg, J.R. (1995). Reactivation of phosphorylated actin depolymerizing factor and identification of the regulatory site. J. Biol. Chem. *270*, 17582–17587.

Ahern-Djamali, S.M., Comer, A.R., Bachmann, C., Kastenmeier, A.S., Reddy, S.K., Beckerle, M.C., Walter, U., and Hoffmann, F.M. (1998). Mutations in Drosophila enabled and rescue by human vasodilator-stimulated phosphoprotein (VASP) indicate important functional roles for Ena/VASP homology domain 1 (EVH1) and EVH2 domains. Mol. Biol. Cell *9*, 2157–2171.

Aizawa, H., Wakatsuki, S., Ishii, A., Moriyama, K., Sasaki, Y., Ohashi, K., Sekine-Aizawa, Y., Sehara-Fujisawa, A., Mizuno, K., Goshima, Y., and Yahara, I. (2001). Phosphorylation of cofilin by LIM-kinase is necessary for semaphorin 3A-induced growth cone collapse. Nat. Neurosci. *4*, 367–373.

Arber, S., Barbayannis, F.A., Hanser, H., Schneider, C., Stanyon, C.A., Bernard, O., and Caroni, P. (1998). Regulation of actin dynamics through phosphorylation of cofilin by LIM-kinase. Nature *393*, 805–809.

Awasaki, T., Saito, M., Sone, M., Suzuki, E., Sakai, R., Ito, K., and Hama, C. (2000). The *Drosophila* trio plays an essential role in patterning of axons by regulating their directional extension. Neuron *26*, 119–131.

Bamburg, J.R. (1999). Proteins of the ADF/cofilin family: essential regulators of actin dynamics. Annu. Rev. Cell Dev. Biol. *15*, 185–230.

Barrett, K., Leptin, M., and Settleman, J. (1997). The Rho GTPase and a putative RhoGEF mediate a signaling pathway for the cell shape changes in Drosophila gastrulation. Cell *91*, 905–915.

Bellanger, J.M., Lazaro, J.B., Diriong, S., Fernandez, A., Lamb, N., and Debant, A. (1998). The two guanine nucleotide exchange factor domains of Trio link the Rac1 and the RhoA pathways in vivo. Oncogene *16*, 147–152.

Billuart, P., Winter, C.G., Maresh, A., Zhao, X., and Luo, L. (2001). Regulating axon branch stability: the role of p190 RhoGAP in repressing a retraction signaling pathway. Cell *107*, 195–207.

Brand, A.H., and Perrimon, N. (1993). Targeted gene expression as a means of altering cell fates and generating dominant phenotypes. Development *118*, 401–415.

Carlier, M.F., Laurent, V., Santolini, J., Melki, R., Didry, D., Xia, G.X., Hong, Y., Chua, N.H., and Pantaloni, D. (1997). Actin depolymerizing factor (ADF/cofilin) enhances the rate of filament turnover: implication in actin-based motility. J. Cell Biol. *136*, 1307–1322.

Chen, J., Godt, D., Gunsalus, K., Kiss, I., Goldberg, M., and Laski, F.A. (2001). Cofilin/ADF is required for cell motility during Drosophila ovary development and oogenesis. Nat. Cell Biol. *3*, 204–209.

Dawe, H.R., Minamide, L.S., Bamburg, J.R., and Cramer, L.P. (2003). ADF/cofilin controls cell polarity during fibroblast migration. Curr. Biol. *13*, 252–257.

Eden, S., Rohatgi, R., Podtelejnikov, A.V., Mann, M., and Kirschner, M.W. (2002). Mechanism of regulation of WAVE1-induced actin nucleation by Rac1 and Nck. Nature *418*, 790–793.

Edwards, D.C., Sanders, L.C., Bokoch, G.M., and Gill, G.N. (1999). Activation of LIM-kinase by Pak1 couples Rac/Cdc42 GTPase signaling to actin cytoskeletal dynamics. Nat. Cell Biol. *1*, 253–259.

Endo, M., Ohashi, K., Sasaki, Y., Goshima, Y., Niwa, R., Uemura, T., and Mizuno, K. (2003). Control of growth cone motility and morphology by LIM kinase and Slingshot via phosphorylation and dephosphorylation of cofilin. J. Neurosci. *23*, 2527–2537.

Etienne-Manneville, S., and Hall, A. (2002). Rho GTPases in cell biology. Nature *420*, 629–635.

Fan, X.P., Labrador, J.P., Hing, H., and Bashaw, G.J. (2003). Slit stimulation recruits Dock and Pak to the roundabout receptor and increases Rac activity to regulate axon repulsion at the CNS midline. Neuron *40*, 113–127.

Fehon, R., Oren, T., LaJeunesse, D.R., Melby, T.E., and McCartney, B.M. (1997). Isolation of mutations in the Drosophila homologues of the human *Neurofibromatosis 2* and yeast *CDC42* genes using a simple and efficient reverse-genetic method. Genetics *146*, 245–252.

Forscher, P., and Smith, S.J. (1988). Actions of cytochalasins on the organization of actin filaments and microtubules in a neuronal growth cone. J. Cell Biol. *107*, 1505–1516.

Fritz, J.L., and VanBerkum, M.F. (2002). Regulation of rho family GTPases is required to prevent axons from crossing the midline. Dev. Biol. *252*, 46–58.

Ghosh, M., Song, X., Mouneimne, G., Sidani, M., Lawrence, D.S., and Condeelis, J.S. (2004). Cofilin promotes actin polymerization and defines the direction of cell motility. Science *304*, 743–746.

Gitai, Z., Yu, T.W., Lundquist, E.A., Tessier-Lavigne, M., and Bargmann, C.I. (2003). The netrin receptor UNC-40/DCC stimulates axon attraction and outgrowth through enabled and, in parallel, Rac and UNC-115/AbLIM. Neuron *37*, 53–65.

Gunsalus, K.C., Bonaccorsi, S., Williams, E., Verni, F., Gatti, M., and Goldberg, M.L. (1995). Mutations in twinstar, a Drosophila gene encoding a cofilin/ADF homologue, result in defects in centrosome migration and cytokinesis. J. Cell Biol. *131*, 1243–1259.

Hakeda-Suzuki, S., Ng, J., Tzu, J., Dietzl, G., Sun, Y., Harms, M., Nardine, T., Luo, L., and Dickson, B.J. (2002). Rac function and regulation during *Drosophila* development. Nature *416*, 438–442.

Hing, H., Xiao, J., Harden, N., Lim, L., and Zipursky, S. (1999). Pak functions downstream of Dock to regulate photoreceptor axon guidance in *Drosophila*. Cell *97*, 853–863.

Hudson, A.M., and Cooley, L. (2002). A subset of dynamic actin rearrangements in Drosophila requires the Arp2/3 complex. J. Cell Biol. *156*, 677–687.

Joneson, T., McDonough, M., Bar-Sagi, D., and Van Aelst, L. (1996). RAC regulation of actin polymerization and proliferation by a pathway distinct from Jun kinase. Science *274*, 1374–1376.

Kozma, R., Sarner, S., Ahmed, S., and Lim, L. (1997). Rho family GTPases and neuronal growth cone remodelling: relationship between increased complexity induced by Cdc42Hs, Rac1, and acetylcholine and collapse induced by RhoA and lysophosphatidic acid. Mol. Cell. Biol. *17*, 1201–121.

Lamarche, N., Tapon, N., Stowers, L., Burbelo, P.D., Aspenstrom, P., Bridges, T., Chant, J., and Hall, A. (1996). Rac and Cdc42 induce actin polymerization and G1 cell cycle progression independently of $p65^{PAK}$ and the JNK/SAPK MAP kinase cascade. Cell *87*, 519–529.

Lee, T., and Luo, L. (1999). Mosaic analysis with a repressible cell marker for studies of gene function in neuronal morphogenesis. Neuron *22*, 451–461.

Lee, T., Lee, A., and Luo, L. (1999). Development of the *Drosophila* mushroom bodies: sequential generation of three distinct types of neurons from a neuroblast. Development *126*, 4065–4076.

Liebl, E.C., Forsthoefel, D.J., Franco, L.S., Sample, S.H., Hess, J.E., Cowger, J.A., Chandler, M.P., Shupert, A.M., and Seeger, M.A. (2000). Dosage-sensitive, reciprocal genetic interactions between the Abl tyrosine kinase and the putative GEF trio reveal trio's role in axon pathfinding. Neuron *26*, 107–118.

Lundquist, E.A., Reddien, P.W., Hartwieg, E., Horvitz, H.R., and Bargmann, C.I. (2001). Three C. elegans Rac proteins and several alternative Rac regulators control axon guidance, cell migration and apoptotic cell phagocytosis. Development *128*, 4475–4488.

Luo, L. (2000). Rho GTPases in neuronal morphogenesis. Nat. Rev. Neurosci. *1*, 173–180.

Machesky, L.M., and Hall, A. (1997). Role of actin polymerization and adhesion to extracellular matrix in Rac- and Rho-induced cytoskeletal reorganization. J. Cell Biol. *138*, 913–926.

Maekawa, M., Ishizaki, T., Boku, S., Watanabe, N., Fujita, A., Iwamatsu, A., Obinata, T., Ohashi, K., Mizuno, K., and Narumiya, S. (1999). Signaling from Rho to the actin cytoskeleton through protein kinases ROCK and LIM-kinase. Science *285*, 895–898.

Mallavarapu, A., and Mitchison, T. (1999). Regulated actin cytoskeleton assembly at filopodium tips controls their extension and retraction. J. Cell Biol. *146*, 1097–1106.

Meberg, P.J., and Bamburg, J.R. (2000). Increase in neurite outgrowth mediated by overexpression of actin depolymerizing factor. J. Neurosci. *7*, 2459–2469.

Mizuno, T., Tsutsui, K., and Nishida, Y. (2002). Drosophila myosin phosphatase and its role in dorsal closure. Development *129*, 1215–1223.

Morgan, T.E., Lockerbie, R.O., Minamide, L.S., Browning, M.D., and Bamburg, J.R. (1993). Isolation and characterization of a regulated form of actin depolymerizing factor. J. Cell Biol. *122*, 623–633.

Nagata-Ohashi, K., Ohta, Y., Goto, K., Chiba, S., Mori, R., Nishita, M., Ohashi, K., Kousaka, K., Iwamatsu, A., Niwa, R., et al. (2004). A pathway of neuregulin-induced activation of cofilin-phosphatase Slingshot and cofilin in lamellipodia. J. Cell Biol. *165*, 465–471.

Newsome, T., Schmidt, S., Dietzl, G., Keleman, K., Asling, B., Debant, A., and Dickson, B. (2000). Trio combines with dock to regulate Pak activity during photoreceptor axon pathfinding in Drosophila. Cell *101*, 283–294.

Ng, J., Nardine, T., Harms, M., Tzu, J., Goldstein, A., Sun, Y., Dietzl, G., Dickson, B.J., and Luo, L. (2002). Rac GTPases control axon growth, guidance and branching. Nature *416*, 442–447.

Niwa, R., Nagata-Ohashi, K., Takeichi, M., Mizuno, K., and Uemura, T. (2002). Control of actin reorganization by Slingshot, a family of phosphatases that dephosphorylate ADF/cofilin. Cell *108*, 233–246.

Ohashi, K., Hosoya, T., Takahashi, K., Hing, H., and Mizuno, K. (2000). A Drosophila homolog of LIM-kinase phosphorylates cofilin and induces actin cytoskeletal reorganization. Biochem. Biophys. Res. Commun. *276*, 1178–1185.

Pollard, T.D., Blanchoin, L., and Mullins, R.D. (2000). Molecular mechanisms controlling actin filament dynamics in nonmuscle cells. Annu. Rev. Biophys. Biomol. Struct. *29*, 545–576.

Prokopenko, S.N., Brumby, A., O'Keefe, L., Prior, L., He, Y., Saint, R., and Bellen, H.J. (1999). A putative exchange factor for Rho1 GTPase is required for initiation of cytokinesis in Drosophila. Genes Dev. *13*, 2301–2314.

Sone, M., Hoshino, M., Suzuki, E., Kuroda, S., Kaibuchi, K., Nakagoshi, H., Saigo, K., Nabeshima, Y., and Hama, C. (1997). Still life, a protein in synaptic terminals of Drosophila homologous to GDP-GTP exchangers. Science *275*, 543–547.

Sone, M., Suzuki, E., Hoshino, M., Hou, D.M., Kuromi, H., Fukata, M., Kuroda, S., Kaibuchi, K., Nabeshima, Y., and Hama, C. (2000). Synaptic development is controlled in the periactive zones of Drosophila synapses. Development *127*, 4157–4168.

Strasser, G.A., Rahim, N.A., VanderWaal, K.E., Gertler, F.B., and Lanier, L.M. (2004). Arp2/3 is a negative regulator of growth cone translocation. Neuron *43*, 81–94.

Strutt, D.I., Weber, U., and Mlodzik, M. (1997). The role of RhoA is tissue polarity and Frizzled signaling. Nature *387*, 292–295.

Svitkina, T.M., and Borisy, G.G. (1999). Arp2/3 complex and actin depolymerizing factor cofilin in dendritic organization and treadmilling of actin filament array in lamellipodia. J. Cell Biol. *145*, 1009–1026.

Wills, Z., Bateman, J., Korey, K.A., Comer, A., and Van Vactor, D. (1999a). The tyrosine kinase Abl and its substrate enabled collaborate with the receptor phosphatase Dlar to control motor axon guidance. Neuron *22*, 301–312.

Wills, Z., Marr, L., Zinn, K., Goodman, C.S., and Van Vactor, D. (1999b). Profilin and the Abl tyrosine kinase are required for motor axon outgrowth in the Drosophila embryo. Neuron *22*, 291–299.

Winter, C.G., Wang, B., Ballew, A., Royou, A., Karess, R., Axelrod, J.D., and Luo, L. (2001). *Drosophila* Rho-associated kinase (Drok) links Frizzled-mediated planar cell polarity signaling to the actin cytoskeleton. Cell *105*, 81–91.

Yang, N., Higuchi, O., Ohashi, K., Nagata, K., Wada, A., Kangawa, K., Nishida, E., and Mizuno, K. (1998). Cofilin phosphorylation by LIM-kinase 1 and its role in Rac-mediated actin reorganization. Nature *393*, 809–812.

Zallen, J.A., Cohen, Y., Hudson, A.M., Cooley, L., Wieschaus, E., and Schejter, E.D. (2002). SCAR is a primary regulator of Arp2/3-dependent morphological events in Drosophila. J. Cell Biol. *156*, 689–701.